

# Characterization of novel 1,3-bis-(*p*-iminobenzoic acid) indane Langmuir-Blodgett (LB) films, with and without $Zn^{2+}$ ions

T. UZUNOĞLU<sup>\*</sup>, H. SARI<sup>a</sup>, R. ÇAPAN, H. NAMLI<sup>b</sup>, O. TURHAN<sup>b</sup>

Balıkesir University, Faculty of Science, Department of Physics, 10100 Balıkesir, Turkey

<sup>a</sup>Ankara University, Faculty of Engineering, Department of Engineering Physics, 06100 Tandogan, Ankara, Turkey

<sup>b</sup>Balıkesir University, Faculty of Science, Department of Chemistry, 10100 Balıkesir, Turkey

Y-type 1,3-bis-(*p*-iminobenzoic acid) indane thin films with and without  $Zn^{2+}$  ions were grown by a LB technique to investigate the influence of the  $Zn^{2+}$  ions on their electrical properties. In this work, 1,3-bis-(*p*-iminobenzoic acid) indane molecules were deposited onto quartz crystal, glass and aluminium coated glass substrates, for optical and electrical measurements. A Quartz Crystal Microbalance (QCM) technique was used to monitor the reproducibility of the film growth. UV-visible spectroscopy was used to verify film deposition. From the electrical measurements, it was observed that  $Zn^{2+}$  ions affect the electrical properties of the LB films, by reducing the barrier height.

(Received November 5, 2008; accepted December 15, 2008)

**Keywords:** 1,3-bis-(*p*-iminobenzoic acid) indane, Langmuir-Blodgett (LB) thin films,  $Zn^{2+}$  ions, Electrical properties

## 1. Introduction

The Langmuir-Blodgett (LB) film technique is a very powerful method for fabricating ultrathin organic films with highly ordered structures [1, 2].

In order to understand the growth process of II-VI semiconductor nanoparticles such as ZnS, CdS etc. in organic thin films, it is essential to know the interaction between metal ions and organic films. Watanabe et al. [3] studied the interactions between conducting LB films and different transition-metal ions ( $Ni^{2+}$ ,  $Cd^{2+}$ ,  $Cu^{2+}$  and  $Zn^{2+}$ ) for chemical sensors. Jung et al. [4] investigated electrical properties for monolayer LB films of pure G4-48PyP dendrimer and its complex with metal ions ( $Pt^{4+}$  and  $Fe^{2+}$  ions). The  $I-V$  characteristics of metal/dendrimer LB film/metal and metal/dendrimer LB films with complex metal ion/metal sandwich structures were measured.  $I-V$  measurements showed that there is a difference between the pure G4-48PyP dendrimer LB film and its complex metal ions [4].

The pyroelectrical activity in copolysiloxane/eicosylamine alternate layer Langmuir-Blodgett (LB) films incorporating  $Cd^{2+}$  and  $Mn^{2+}$  ions was reported and the pyroelectric results showed that cadmium ion incorporation caused a considerably improved performance compared to the system without metal ions [5].

In this study, Y-type LB films of 1,3-bis-(*p*-iminobenzoic acid) indane (IBI) thin films with and without  $Zn^{2+}$  ions were deposited onto quartz crystal, microscope glass and aluminium coated microscope to fabricate a metal/Y-type LB film/metal device in order to investigate the influence of  $Zn^{2+}$  ions on the electrical

properties of 1,3-bis-(*p*-iminobenzoic acid) indane molecules.

## 2. Experimental details

The chemical structure of IBI is shown in Fig. 1. It was dissolved in a 9:1 ratio of chloroform and methanol. The zinc chloride was dissolved in the subphase and a  $0.5 \text{ mg ml}^{-1}$  concentration of the solution was used to take an isotherm and to produce a LB film by spreading onto a pure water surface. A time period of 15 minutes was allowed for the solvent to evaporate before the area enclosed by the barriers was reduced. The transfer speed onto an aluminised glass substrate was  $10 \text{ mm min}^{-1}$ , and a deposition pressure of  $20 \text{ mN/m}$  was selected to produce Y-type LB films having thicknesses of 5 and 11 monolayer IBI samples, with and without  $Zn^{2+}$  ions, by vertically dipping substrates into the solution.

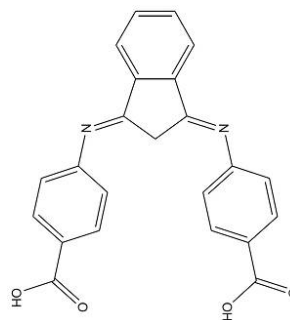


Fig. 1. Chemical structure of 1,3-bis-(*p*-iminobenzoic acid) indane.

The temperature of the water subphase was controlled using a Lauda Ecoline RE 204 temperature control unit, and all experimental data were taken at room temperature.

In this study, QCM measurements were performed at room temperature using an in-house designed oscillating circuit and standard quartz crystal with a nominal resonance frequency of 9 MHz. The frequency was measured with a MOTECH FG-513 function generator and a TEKTRONIX TDS 210 digital oscilloscope.

Microscope glass and aluminised microscope glass were used for optical and electrical measurements, respectively. The films were grown on Al-coated glass placed into a thermal evaporator for top electrode fabrication. Top electrodes of the films were fabricated under  $8 \times 10^{-7}$  mbar vacuum by evaporating aluminium using a mask which had 16 parallel; 1mm $\times$ 15mm sized opening interdigitated grids on it. The Metal/LB films/metal sandwich structure is shown Fig. 2.

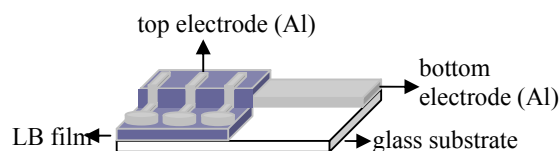


Fig. 2. The device structure of the LB film for electrical measurements.

Optical measurements were carried out with a Perkin Elmer Lambda-2 UV-VIS spectrometer. For electrical measurements, a HP 4192A impedance analyzer, a Keithley 228A current source, a Keithley 6514 voltmeter and a Keithley 485 ampermeter were used. All the data were taken automatically using a GPIB interface card and LABVIEW data acquisition software.

### 3. Experimental results

Fig. 3 shows the change in the resonant frequency as a function of the number of deposited layers, for films with and without Zn<sup>2+</sup> ions [6]. In order to understand the LB film quality, the relation between the frequency change and mass change is analyzed. A quartz crystal with electrodes on both sides will resonate at an extremely well-defined frequency when placed in a suitable electronic control unit. The resonant frequency depends on the area of the electrode and the thickness of the quartz crystal. The resonant frequency of the crystal is extremely sensitive to small mass changes. The change in resonant frequency,  $f$ , has been shown to be directly proportional to the mass deposition on the quartz crystal, and this relation for LB films can be given by

$$\Delta f = \frac{2f_0^2 \Delta m}{K_q} N \quad (1)$$

where  $f_0$  is the initial oscillation frequency,  $K_q = \rho_q v_q$ ,  $\rho_q$  is the density of the piezoelectric slab,  $v_q$  is the propagation speed of acoustic waves in the quartz,  $N$  is the number of deposition layers,  $\Delta m$  is the mass per unit area per layer [7].

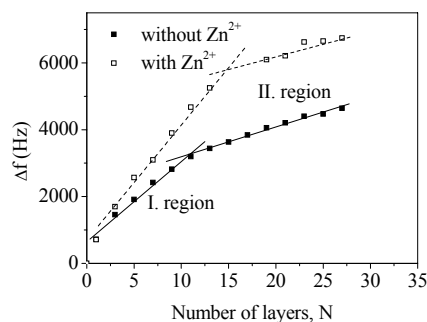


Fig. 3. Plots of measured frequency change to layer numbers of Y-type IBI LB films, with and without Zn<sup>2+</sup> ions.

In Fig. 3, two linear regions can be seen in the Y-type IBI samples, with and without Zn<sup>2+</sup> ions. In the first region, the slope of this graph shows that the frequency changes,  $\Delta f$  are 253 Hz and 355 Hz per bilayer, respectively. The masses deposited on the quartz crystal per bilayer can be calculated as 291 ng and 408 ng, using eq. 1. In the second region, the  $\Delta f$  values are found to be 89 Hz and 70 Hz per bilayer. The masses deposited on the quartz crystal per bilayer can be calculated as 102.5 ng and 81 ng. Other results have been reported for  $\alpha$ -pinene molecules (for a molar ratio 1:0.1 C<sub>20</sub>/C<sub>60</sub>). The frequency shift decreased when the number of layers was greater than 10 [8]. From Fig. 3, the two linear regions explain that with and without Zn<sup>2+</sup> ions, the IBI film mass depositions onto the quartz crystal in the second region were lower than in the first region.

Fig. 4 shows the UV absorption spectra of the 5, 11 and 15 monolayer IBI films, with and without Zn<sup>2+</sup> ions [9]. Monolayer growth on the substrate was verified using UV-Vis spectra. When the number of layers was increased, the intensities of absorption peaks decreased, showing the monolayer growth on the substrate.

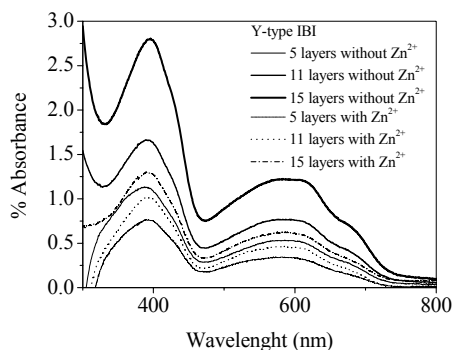


Fig. 4. UV-visible absorption spectra of with and without Zn<sup>2+</sup> ions for Y-type IBI LB films with different numbers of layers.

The electrical properties of the films were investigated by measuring the room temperature I-V characteristics. Fig. 5 shows I-V curves of the 5 and 11 layer, with and without  $Zn^{2+}$  ions [9], IBI samples. The I-V curves show exponential behaviour, and regardless of film thickness there is a decrease in the current for the samples containing  $Zn^{2+}$  ions, as compared to the samples without  $Zn^{2+}$  ions.

Although this increase is small, it is consistent with other reported results observed for G4-48PyP dendrimer LB films and their  $Fe^{2+}$  ions [4].

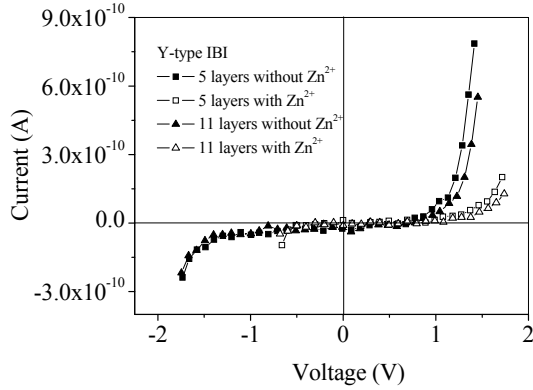


Fig. 5. Room temperature I-V graph of the films without  $Zn^{2+}$  IBI (■, ▲) and with  $Zn^{2+}$  IBI (□, △).

In order to explain the conduction process through LB films and the effect of the  $Zn^{2+}$  ions on the conductivity,  $\ln J$  versus  $V^{1/2}$  has been plotted in Fig. 6 for 5 and 11 layer thick samples, in the voltage range corresponding to the exponentially increasing current. As seen from Fig. 6, the relationship between  $\ln J$  and  $V^{1/2}$  shows a rather linear dependence.

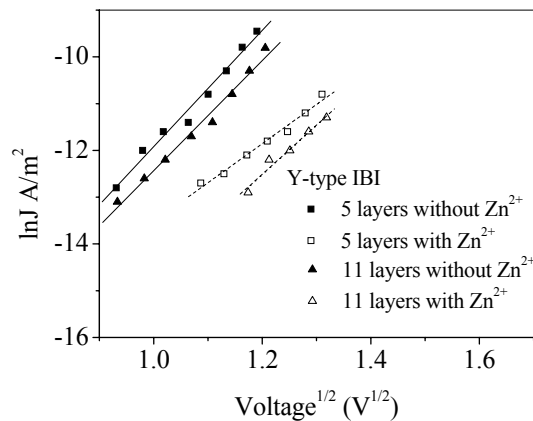


Fig. 6. Plot of  $\ln J$  versus  $V^{1/2}$  for various number of without  $Zn^{2+}$  IBI layers (■, ▲) and with  $Zn^{2+}$  IBI (□, △).

The linear dependence suggests that conduction is governed by either a Poole-Frenkel or a Schottky mechanism [10]. We can make basic assumptions and extract some physically acceptable information. Let us

assume that conduction is governed by the Schottky conduction mechanism, which is given by [11]

$$I_{Schottky} = A.S.T^2 \exp\left(\frac{-e\phi}{kT} + \beta V^{1/2}\right) \quad (2)$$

where  $A$  is the Richardson constant,  $S$  is the metal contact area,  $T$  is absolute temperature,  $e$  is the electronic charge,  $k$  is the Boltzmann's constant,  $\phi$  is the potential barrier height,  $V$  is the applied voltage, and  $\beta$  is the Poole-Frenkel field-lowering coefficient given by

$$\beta_{PF} = \frac{e}{kT} \left( \frac{e}{\pi\epsilon_0\epsilon_r d} \right)^{1/2} \quad (3)$$

here,  $\epsilon_r$  is the dielectric constant of the film;  $\epsilon_0$  is the permittivity of free space,  $d$  is the film thickness.

The intercept of the linear curve with the  $\ln J$  axis at  $V=0$  can then be expressed in terms of the barrier height ( $\phi$ ) and temperature, using Eq. 2:

$$\ln J = \ln(AT^2) - \left(\frac{e}{kT}\right)\phi \quad (4)$$

The results of the barrier height calculation of the 5 and 11 monolayer thick samples, with and without  $Zn^{2+}$  ions, are summarized in Table 1. From this, the 5 and 11 monolayer thick samples without  $Zn^{2+}$  ions have slightly different barrier heights than the 5 and 11 monolayer thick ones with  $Zn^{2+}$  ions [4].

Table 1. Calculation details for the barrier height energy.

Molecules	Number of layers	$\ln J$ (V=0)	Barrier height $\phi$ (eV)
without $Zn^{2+}$ IBI	5	-24.3	1.25
	11	-24.2	1.25
with $Zn^{2+}$ IBI	5	-21.9	1.19
	11	-25.0	1.27

#### 4. Conclusions

In this paper, Y-type IBI samples with and without  $Zn^{2+}$  ions were grown in various layer thicknesses on quartz crystal glass and aluminized substrates, using a LB technique. The samples, which had different numbers of layers, were checked using a QCM technique and UV-Vis spectra. The QCM results showed that for 11 and 15 monolayer thick IBI samples, without and with  $Zn^{2+}$  ions, the transfer ratio was very low. By assuming a Schottky conduction mechanism, the average LB film/barrier height was found to be 1.23 eV for IBI samples with  $Zn^{2+}$  ions and 1.25 eV for those without  $Zn^{2+}$  ions, respectively.

### Acknowledgements

Financial support from Ankara University Research Office (BAP) (Project code: AU-BAP 2003-07-45-016) is gratefully acknowledged. The authors also would like to thank S. Uzun, and S. Durkut for their help.

### References

- [1] G. G. Roberts, Langmuir-Blodgett Films, Plenum Press, New York, 1990.
- [2] M. C. Petty, Langmuir-Blodgett Films: An Introduction, Cambridge University Press, Cambridge, 1996.
- [3] N. Watanabe, H. Ohnuki, M. Izumi, T. Imakubo, Colloids and Surfaces A: Physicochem. Eng. Aspects **284-285**, 640 (2006).
- [4] S. B. Jung, C. Kim, Y. S. Kwon, Thin Solid Films **438-439**, 27 (2003).
- [5] R. Çapan, T. Richardson, D. Lacey, Thin Solid Films, **327-329**, 369 (1998).
- [6] T. Uzunoğlu, Investigation of the Properties of Organic LB Thin Films Consisting Semiconducting II-VI Group Nanoparticles, Ph. D. Thesis, Turkey 53, 2008.
- [7] R. Çapan, M. Evyapan, H. Namlı, O. Turhan, G. A. Stanciu, Journal of Nanoscience and Nanotechnology **5**, 1108 (2005).
- [8] S. S. Shiratori, M. Shimizu, K. Ikezaki, Thin Solid Films **327-329**, 655 (1998).
- [9] H. Sarı, T. Uzunoğlu, O. Turhan, BAÜ Fen Bil. Enst. Dergisi **8**(1) 46 (2006).
- [10] N. J. Geddes, J. R. Sambles, W. G. Parker, N. R. Couch, D. J. Jarvis, J. Phys. D. Appl. Phys. **23**, 95 (1990).
- [11] S. M. Sze, Physics of Semiconductor Devices, Wiley-Interscience, New York, 250, 1981.

Corresponding author: utayfun@gmail.com